Electrical Switch for Smart pH Self-Adjusting System Based on Silver Nanowire/Polyaniline Nanocomposite Film

Gui-Wen Huang,[†,‡] Hong-Mei Xiao,[†] and Shao-Yun Fu[*,†]

[†]Technical Institute of Physics and Chemistry, Chinese Academy of Sciences, No. 2 Beiyitiao, Zhongguancun, Beijing 100190, PR China and [‡]University of Chinese Academy of Sciences, Beijing 100039, PR China

ABSTRACT

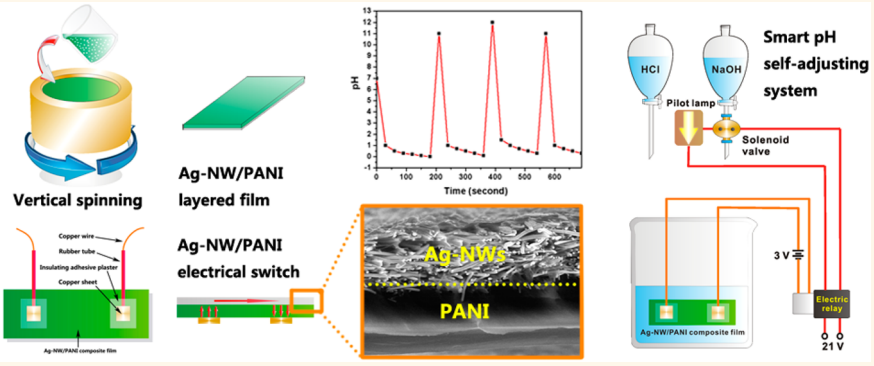

A sensitive pH-triggered electrical switch is demonstrated by using a layer-structured silver nanowire/polyaniline nanocomposite film fabricated *via* an easy vertical spinning method. The as-prepared nanocomposite film shows the high electrical conductivity of 1.03×10^4 S cm^{-1} at the Ag-NW areal density of 0.84 mg cm^{-2} and a good cycling stability. Particularly, because of the layered structure, the switch achieves a very high contrast ratio of *ca.* 9×10^8, which is 2−6 orders higher than that reported previously. The high electrical conductivity and the high switching ratio make the layer-structured nanocomposite film a sensitive switch candidate for pH-responsive systems. Finally, a smart pH self-adjusting switching system is successfully designed using the as-prepared layer-structured nanocomposite film.

KEYWORDS: smart material · silver nanowire · polyaniline · composite film · pH

"Smart materials" that respond to their environmental/external stimuli to produce a dynamic and reversible change in properties[1] have recently received great interest due to their promising applications in sensors,[2,3] display technologies,[4,5] drug delivery,[6,7] bioengineering,[8,9] *etc.* The external stimuli include environmental pH,[10] thermo,[11] photo,[12] electro,[13] magnetic[14] stimuli and so on. Of them, pH is an important external stimulus factor because it plays significant roles in chemical reactions for general chemistry, biochemistry, clinical chemistry or environmental science; moreover, numerous life processes are also found to be closely related to the pH value.[10,15] Various pH-responsive materials have been developed from organic/inorganic nanoparticles[16−20] to polymer cluster or complexes.[21−24] These materials are generally in nanoscale powder forms.[16,17,19,21] However, in many practical applications such as electrodes in cells *etc.*, the free-standing robust bulk materials rather than powders are required.[25−27] Consequently, conducting polymers (CPs) are assumed as promising candidates for pH-responding materials. This is because on the one hand, they contain atoms that are prone to protonation,[10,28] which provides their ability of pH-response; on the other hand, CPs can be easily fabricated into free-standing bulk films.[29,30] Since

* Address correspondence to syfu@mail.ipc.ac.cn.

Received for review January 16, 2015 and accepted February 25, 2015.

Published online February 25, 2015
10.1021/acsnano.5b00348

size and thickness of the polymer-based free-standing films can be easily controlled in an exact way, it enables them to suit various application situations.[31,32] Among CPs, PANI owns many excellences such as low cost, easy synthesis, outstanding environmental stability and well-controllable physical properties.[33−35] More importantly, it shows great potential in pH response for its outstanding reversible doping/dedoping performance.[10,36] In an acid/base chemistry, its electrical and photorelative characteristics vary dramatically between doped and dedoped form.[10,37−40] Several PANI-based pH-switching smart materials have been reported to demonstrate switchable properties in luminescence,[10] chemoelectrical polarity[39] and photo absorption[28] as responding signals. Compared with these responding signals, electrical signal possesses greater usability since electronics have become mainstays of many applications in modern society and the electrical signal can directly drive electronics to execute actions in the smart systems, leading to higher speed and efficiency of operation.[41,42] Furthermore, electrical signal response could be exploited for many novel applications such as switching and transistor actions, logic gates and data memories.[43,44] Therefore, it is of great practical importance to develop PANI-based pH-switching materials that respond sensitively to electrical signals.

The EC of PANI in doped form is in the level of $\sim 10^0$ S cm^{-1},[45−47] which is far below the required EC for practical applications in electrical systems.[48−50] This is possibly why PANI-based electrical switches have been rarely reported yet. Actually, a reasonably high EC of $\sim 10^4$ S cm^{-1} closing to that of eutectic solders commonly used in applied circuits[49] is usually required so that the rated currents of the electrical components can be achieved under a universal voltage.[48,50] Therefore, the EC of the PANI-based materials has to be greatly improved in order to apply them to electrical systems. Addition of conductive fillers to polymer matrix is proven to be an easy but effective way for enhancing the EC of the polymer composites. Conductive fillers such as carbon nanotubes[51−53] and graphene[54−56] have been employed to fabricate PANI-based composites, but the improvement of the EC by these fillers are quite limited (about 10 S cm^{-1}).[51−56] This was mainly attributed to the large contact resistance among the carbon fillers. The contact resistance of the carbon-based materials is rather huge compared to metals,[57] which results in the much lower EC of the composites than expected. By contrast, silver nanowires (Ag-NWs) are the ideal conducting filler for enhancing the EC of the polymers. First, Ag possesses the highest EC among metals; second, Ag is fairly resistant to corrosion, which is important for serving in environments with various pH values; third, the high aspect ratio of Ag-NWs is another important advantage in forming electrically conducting networks in composites.[50,58] Therefore, in this work, Ag-NWs will be chosen as conductive fillers to fabricate conductive PANI-based composite films to make sensitive pH-triggered electrical switching systems.

It should be emphasized here that as an electrical pH-responsive material, the conductivity should be reversibly switched by the change of pH. And a high contrast ratio in electrical property between doped and dedoped form and thus a high switching ratio is desired for a high performance switch with a high sensitivity so that the high conductivity contrast ratio will make the system sensitive and effective.[59,60] Conductive fillers are usually uniformly dispersed in the PANI matrix to improve the EC.[29,61,62] However, the addition of conductive fillers to PANI matrix normally leads to the reduction of switching ratio since the electrical property of the uniform-structured composite in dedoped form will also be greatly enhanced by the conductive fillers.[29,62,63] Herein a layer-structured composite film is intentionally designed for the purposes of not only greatly enhancing the EC in doped form but also increasing the electrical switching ratio between dedoped and doped forms. Through an easy vertical spinning (VS) process, the layer-structured composite films of a high pH-sensing PANI layer and an ultrahigh EC Ag-NW layer are prepared. The PANI layer apparent EC of the nanocomposite film can be reversibly switched by adjusting the external pH and be greatly enhanced in its doped form by the Ag-NW layer while not obviously influenced in dedoped form, bringing about a very high switching ratio. The as-prepared nanocomposite film shows the high electrical conductivity of 1.03×10^4 S cm^{-1} at the Ag-NW areal density of 0.84 mg cm^{-2} and an excellent cycling stability. The high electrical conductivity and the high contrast ratio make the layer-structured nanocomposite film as a superswitch candidate with an excellent sensitivity for pH-responsive systems. Finally, a smart pH self-adjusting switching system is successfully designed using the as-prepared layer-structured nanocomposite film. Particularly, the switching system achieves a very high contrast ratio of *ca.* 9×10^8 due to the layered structure of the nanocomposite film, which is much higher than that reported in the literatures.[31,32,63,64]

RESULTS AND DISCUSSION

The original VS process is developed as shown in Figure 1. Ag-NWs are first dispersed in PANI-*N*-methyl-2-pyrrolidone (NMP) solution by a bath sonicator to form a uniform mixture. The resultant mixture is then poured into a barrel-like container made of Stainless Steel 304 (06Cr18Ni9). The container is coaxially rotated at a high speed of 2000 r min^{-1} by a motor. The container has a vertical inside wall and an annular baffle on the top. Because of the great centrifugal force under a high speed rotation, the mixture is spread to form a uniform liquid film along the inside wall of the

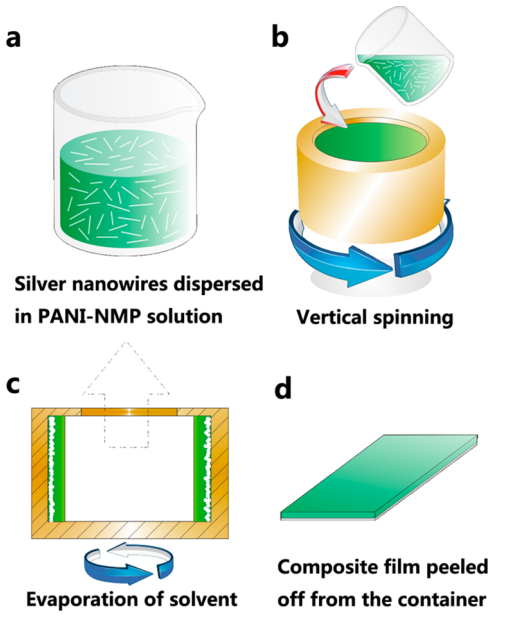

Figure 1. Schematic diagram of the vertical spinning method: (a) prescribed silver nanowires are dispersed in PANI-NMP solution to form uniform mixture, (b) the resultant mixture is poured into a high speed rotating barrel-like container, (c) the rotating container is heated to evaporate the solvent and (d) the final nanocomposite film is obtained by peeling it off from the inside wall of the container.

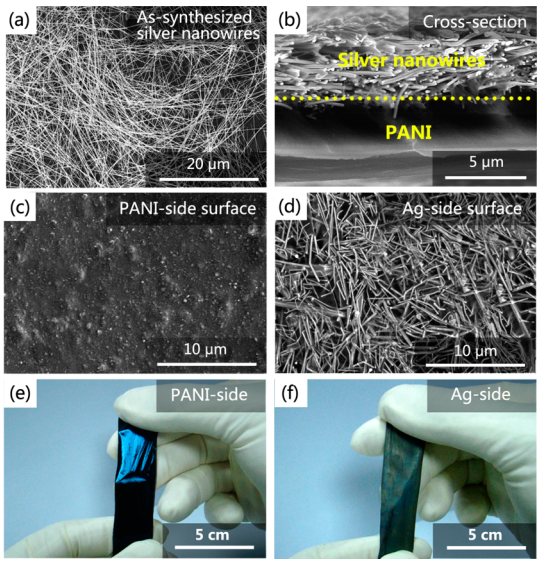

Figure 2. (a) SEM image of the synthesized silver nanowires, (b) SEM image for the cross-section of the Ag-NW/PANI composite film (AD = 0.84 mg cm^{-2}), (c) SEM image for the surface of the PANI-side of the composite film, (d) SEM image for the surface of the Ag-side of the composite film, in which the Ag-NW AD of the film is 0.84 mg cm^{-2}, (e) digital photograph of the PANI-side and (f) digital photograph of the Ag-side of the composite film.

container. Afterward, the container is heated to evaporate the solvent, and the rotation maintains throughout the whole evaporation procedure. Since the density (10.5 g cm^{-3}) of Ag-NW is much higher than that (1.2 g cm^{-3}) of PANI, Ag-NWs will be centrifuged to the outside of the film during rotation, forming a layer-structured composite film. The composite film can be easily peeled off after immersing in water from the inside of the container.

The as-synthesized Ag-NWs used in the present work are displayed in Figure 2a. The details of the length and diameter distributions of the Ag-NWs are shown in Figure S1 (Supporting Information). Figure 2b shows the scanning electronic microscopy (SEM) image of the cross-section of the nanocomposite film with an Ag-NW AD of 0.84 mg cm^{-2}. The content of the Ag-NWs in the composite film is described by an areal density (AD), namely the Ag-NWs weight in per unit area of the composite films. From the SEM image, it can be seen that the Ag-NWs are present only in the Ag-side. This will keep the PANI-side of the composite film in an insulating state in its dedoped form. A clear boundary between the PANI layer and the Ag-NW layer can be seen. The thickness is about 2.5 μm for the Ag-NW layer and is about 10 μm for the PANI layer.

Ag-NWs in the layer-structured composite film are tightly stacked due to the centrifugal force. This ensures the good contact among Ag-NWs, leading to an excellent electrical property of the Ag-NW network. The layered structure makes the composite film an excellent candidate as a switch: the PANI layer provides a pH-sensing functionality while the Ag-NW layer supplies a high conductivity when PANI is in the doped form. Figure 2c and 2d are the corresponding SEM images of the surfaces of the two sides. Figure 2e and 2f shows the digital photographs of the PANI-side and the Ag-side of the as-prepared layer-structured composite film, respectively.

Since the composite film has a layered-structure, the sheet resistance of its two sides will be different. The bulk conductivity of the composite film and the sheet resistances of both sides of the films are respectively tested following the methods schematically shown in Figure 3a. Figure 3b shows the bulk conductivity of the composite film as a function of the Ag-NW AD, in which all the samples consist of the same areal density of the PANI (1.2 mg cm^{-2}). It can be seen from Figure 3b that the composite conductivity increases sharply with increasing the Ag-NW AD when it is lower than 0.84 mg cm^{-2}, indicating that the conductive network is being gradually constructed. On the other hand, the conductivity increases relatively slowly with further increasing the Ag-NW AD when it is higher than 0.84 mg cm^{-2}. This is because the continuous network has been built up when the Ag-NW areal density is equal to 0.84 mg cm^{-2} and a further increase of the Ag-NW amount will no longer influence the EC significantly.

Moreover, the conductivity value of 1.03×10^4 S cm^{-1} at the Ag-NW AD of 0.84 mg cm^{-2} is close to that of universal eutectic solders as mentioned above, which can meet there requirements for various electronic applications.[48−50] Therefore, 0.84 mg cm^{-2} is chosen as the proper Ag-NW AD for fabricating Ag-NW/PANI

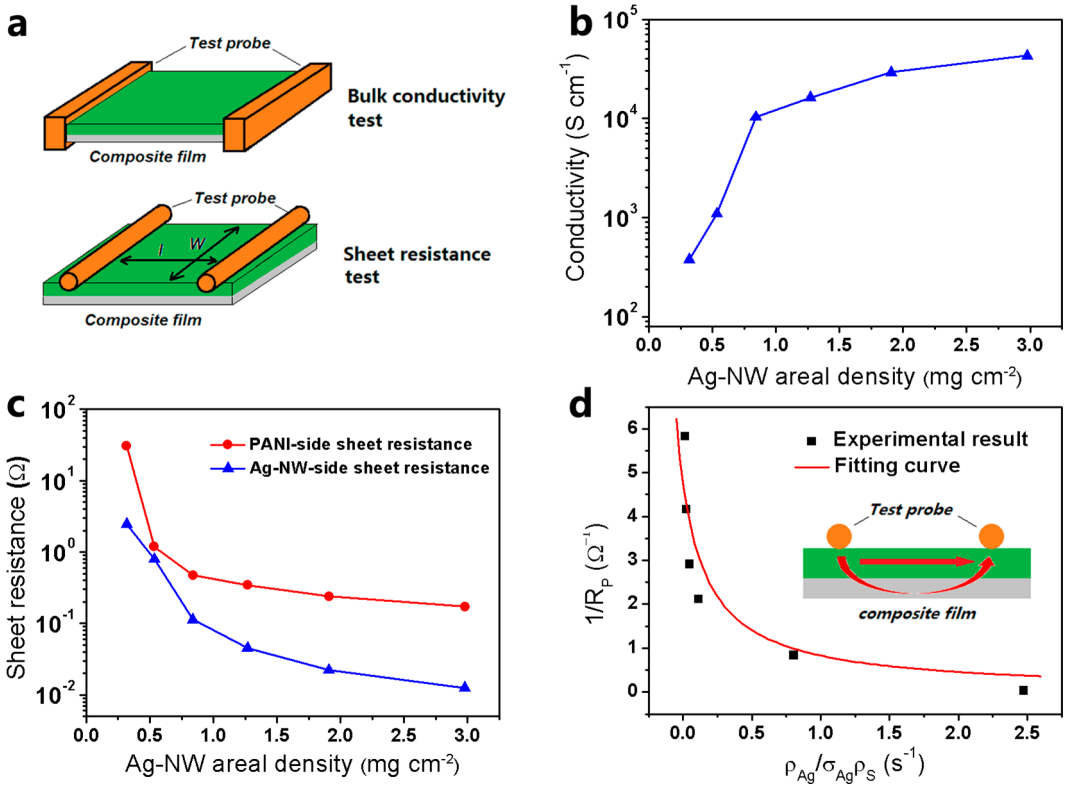

Figure 3. (a) Schematic diagrams for the measurement methods for bulk conductivity and sheet resistance of the Ag-NW/PANI composite film, (b) bulk conductivity of the composite film as a function of the Ag-NW AD, (c) sheet resistance of the PANI and Ag-NW sides of the composite film as a function of the Ag-NW AD and (d) fitting curve of $1/R_P$ against $\rho_{Ag}/\sigma_{Ag}\rho_S$ of the composite film for evaluation of the contact resistance between the two layers. The inset is the schematic diagram of the parallel resistance model of the composite film.

composite film switch. The sheet resistance of the Ag-side and PANI-side of the films is displayed in Figure 3c. As expected, the sheet resistance of the Ag-side decreases dramatically with the increase of Ag-NW AD. More importantly, the sheet resistance of the doped PANI-side also decreases greatly with the increase of Ag-NW AD. This is because the layer-structured composite film can be regarded as a parallel resistance combination of the two layers, and the apparent electrical property of the PANI layer is enhanced by the conductive Ag-NW layer.[64] Thus, the sheet resistance of the PANI side is dramatically reduced due to the parallel combination effect. Besides the high conductivity of the Ag-NW layer, the small contact resistance (R_C) between the two layers is another important reason for the large enhancement of the electrical property in doped form. The R_C is evaluated by considering the layer-structured composite film as a parallel resistance combination model as described in the inset of Figure 3d.[64] According to the parallel resistance law, R_C of the composite film can be obtained from eq 1. The details for the derivation of eq 1 are given in the Supporting Information.

$$\frac{1}{R_P} = \frac{208.3 + \rho_{Ag}/\sigma_{Ag}\rho_S + 2R_C}{208.3\rho_{Ag}/\sigma_{Ag}\rho_S + 416.6R_C} \quad (1)$$

In eq 1, R_P is the sheet resistance of the PANI-side of the layer-structured composite film and σ_{Ag} is the conductivity of the Ag-NW layer. And ρ_S is the areal density of the Ag-NWs in the composite films, while ρ_{Ag} is the bulk density of the Ag-NWs. Thus, R_C can be estimated by fitting the curve of $1/R_P$ against $\rho_{Ag}/\sigma_{Ag}\rho_S$ as shown in Figure 3d. Finally, R_C between the two layers is evaluated to be about 0.11 Ω square^{-1}, which is smaller than that (>0.2 Ω square^{-1}) of the stainless steel-PANI systems.[65] Therefore, the combination of the small contact resistance and the high conductivity of the Ag-NW layer finally results in the outstanding electrical property of the nanocomposite film. However, when the film is in dedoped form, the sheet resistance of the PANI layer is rather huge (>10^6 Ω). For this case, the electrical property of the composite film is mainly determined by the resistance of the PANI layer; thus, the contact resistance between layers is no longer a major influencing factor.

As shown in Figure 4a, when the layer-structured composite film is used as an electrical switch, two copper electrodes are attached on the PANI-side of the composite film by a conductive adhesive and the insulated adhesive plaster is used to isolate the electrodes from the conductive environmental solution. Figure 4b schematically describes how the electrical switch works. The composite film is connected with a powered circuit by a direct current (DC) power supply to build a switch circuit. When the PANI layer is in the

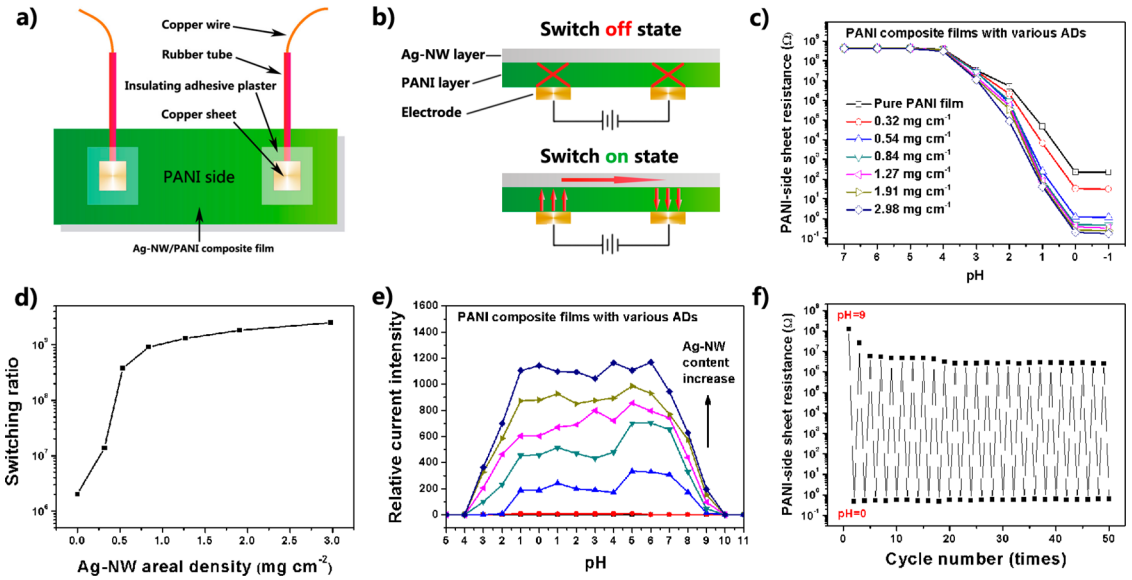

Figure 4. (a) Schematic diagram of the pH-triggered electrical switch based on the layer-structured Ag-NW/PANI films, (b) the "off" and "on" state of the switch corresponding to the dedoped and doped form of the PANI layer, (c) the PANI-side sheet resistance of the Ag-NW/PANI composite films with various Ag-NW ADs as a function of environmental pH, where the pH value is controlled by adjusting the added amount of HCl, (d) switching ratio of the switch as a function of Ag-NW AD, (e) comparison of the current intensity passing through the switches with different Ag-NW ADs as a function of pH when they are powered by the same voltage power supply and (f) PANI-side sheet resistance response of the composite film with an Ag-NW AD of 0.84 mg cm^{-2} upon alternatively adjusting the solution pH value between 0 and 9.

dedoped form, the switch circuit is open due to the nonconductive characteristic of the PANI layer, and the switch shows the "off" state. When the PANI layer is triggered to the doped form by the pH stimulus, the switch circuit is close and the current is allowed to pass through both the conducting PANI layer and the Ag-NW layer, thus the switch shows the "on" state. Therefore, the electrical property of the PANI-side of the composite film is the dominating parameter for the switch. The electrical property of the PANI-side can be described by an apparent sheet resistance. The PANI-side sheet resistance of the composite films is presented in Figure 4c as a function of the Ag-NW AD, in which the pH value is adjusted by the addition of HCl. It can be seen that the PANI-side sheet resistance of the composite film decreases gradually as the pH value decreases, indicating that the PANI is gradually doped by the proton acid. Moreover, the doped PANI-side sheet resistance decreases dramatically with increasing the Ag-NW AD, which indicates that the apparent electrical property of the PANI-side is greatly enhanced by the Ag-NW layer. The ratio of the dedoped PANI-side sheet resistance to that of the doped form is defined as a switching ratio. The switching ratio is an important parameter for a switch and a high switching ratio means that the switch has a high sensitivity and efficiency.[59,60] As shown in Figure 4d, the switching ratio of the composite film is significantly enhanced by the addition of Ag-NWs. Table 1 displays that the switching ratio of the Ag-NW/PANI composite film with an Ag-NW AD of 0.84 mg cm^{-2} is two to six orders higher than that the previously reported PANI-based electrical pH responsive materials.[29,30,62,63] This indicates that the as-prepared layer-structured Ag-NW/PANI nanocomposite film is sensitive to the pH change of the environment.

TABLE 1. Switching Ratio of PANI-Based Electrical pH Responsive Materials

materials	switching ratio	ref no.
Au/PANI	6.0×10^2	63
Gum acacia/PANI	3.2×10^3	62
CNT/PANI	1.5×10^5	29
PANI	8.6×10^6	30
Ag-NW/PANI	9.1×10^8	present work

It can be seen that the switching ratio of the layer-structured Ag-NW/PANI composite film is *ca.* two orders higher than that of the pure PANI and up to 5.5 orders higher than that of uniform composites. By contrast, the switching ratio of the previously reported PANI-based materials[29,30,62,63] is much lower than that of the pure PANI. This is because for these composite materials, their uniform structures make their EC in the dedoped state also greatly enhanced by the conductive fillers, leading to the reduction of the switching ratio, which is an adverse effect for switches. Both the high switching ratio and the high electrical property will allow a great current in the circuit to pass through the composite film in its doped form under universal voltage supplies. Figure 4e shows the comparison of the current intensity passing through the switches with different Ag-NW areal densities as a function of pH when they are powered by the same voltage power

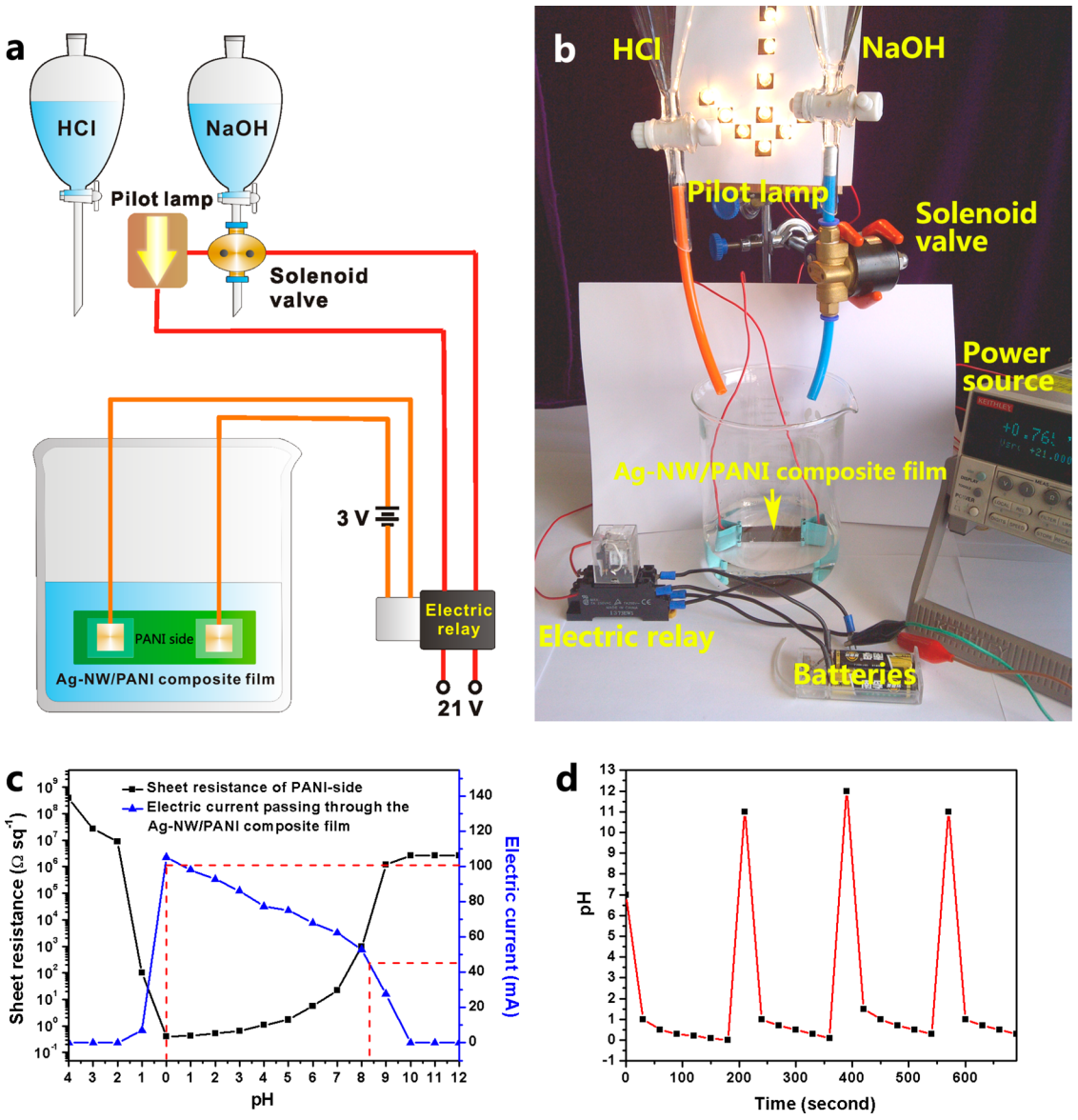

Figure 5. A smart pH self-adjusting system using the Ag-NW/PANI composite film as a pH-triggered electrical switch: (a) schematic diagram of the system; (b) digital photograph of the smart system when it is in its "on" state; (c) the sheet resistance of the PANI-side of the composite film with an Ag-NW AD of 0.84 mg cm^{-2} and the electric current in the switch circuit as a function of the solution pH, the dotted red lines are the "on" (upper) and "off" (lower) current value of the electric relay; (d) the real pH value of the solution in the smart pH self-adjusting system as a function of time.

supply. It can be seen that the current-carrying ability of the switch is dramatically improved by the layered structure of the Ag-NW/PANI composite films. This makes it possible to directly drive electronic devices in smart systems by the switch *via* controlling the current. Figure 4f shows the PANI-side sheet resistance response of the composite film upon alternatively adjusting the solution pH value between 0 and 9. For the first two cycles, the PANI-side sheet resistance of the dedoped form (pH = 9) decreases from 10^8 Ω to 10^7 Ω, and subsequently stabilizes near 10^7 Ω. This decrease results from the incomplete recovery of the protonation upon returning from the doped state.[28] The switching between the doped and dedoped form is robust and maintains a switching ratio in excess of 7 orders after 50 continuous cycles, which shows the excellent cycling stability of the switch.

A smart pH self-adjusting system is demonstrated by using the layer-structured nanocomposite film with an Ag-NW AD of 0.84 mg cm^{-2} as the electrical switch. The system simulates the pH self-adjusting process as the acidity increases continuously, which is schematically described in Figure 5a. HCl is slowly released to the solution and the pH of the solution is then reduced gradually. When the pH reaches the critical value set at (=0), the composite film switch is triggered to its "on" state; at the same time, the electric relay controlled by the composite film is triggered on, and the solenoid valve and pilot lamp are powered. NaOH is then rapidly released by the solenoid valve to neutralize the HCl.

Afterward, the system will then be back to the "off" state when the pH of the solution exceeds the critical value and a new cycle begins.

The working process in Figure 5a is explained here. The switch as shown in Figure 4a is serially connected to an electric relay (resistance = 28 Ω, open current = 100 mA and close current = 45 mA) to build a switch circuit. A power supply with a 3 V voltage is used in the circuit as a permanent potential. Thus, the electric current in the electric relay is controlled by the switch. The film is then immersed in water in a beaker. The environmental pH is adjusted by controlling the amount of HCl aqueous solution (5 M) and NaOH aqueous solution (10 M) added to the beaker. After added to the beaker, the solution is mixed rapidly by a magnetic stirrer. The addition of NaOH is managed by a solenoid valve, which is controlled by the electric relay and powered by a voltage source (Keithley source meter 2400) as well as the pilot lamps. In a typical process, the solution is neutral initially. The PANI layer of the composite film is insulated, namely the switch is in the "off" state. Then, the HCl solution is dripped slowly into the beaker and the dripping is kept throughout the whole process. As the pH is reduced, the PANI layer of the composite film becomes gradually doped, leading to the decrease of the PANI-side resistance; at the same time, the electric current in the switch circuit rises. When the current reaches the current value required for opening the electric relay (100 mA), the system turns to the "switch on" state: the pilot lamp is lit up and the solenoid valve is opened. Then the NaOH solution is released rapidly into the beaker though the solenoid valve. After the addition of NaOH, the pH of the solution rises and the PANI layer is then gradually dedoped, causing the current decrease in the switch circuit. When the current is decreased to the one required for closing the electric relay (45 mA), the system turns back to the "switch off" state and the addition of NaOH is then stopped. Afterward, as the HCl keeps dripping, a new adjusting cycle begins. The system then starts to carry out the pH self-adjusting process repeatedly. Figure 5b shows the digital photo of the system when it is in the "switch on" state. Video S1 in the Supporting Information shows a typical pH self-adjusting process as described above.

Figure 5c shows the sheet resistance of the PANI-side of the composite film and the corresponding electric current in the switch circuit as a function of the solution pH. It can be seen that the sheet resistance decreases dramatically as pH decreases especially below 2. When the pH is decreased to about 0, the current in the switch circuit approaches 100 mA, the system is then triggered to add NaOH to the solution to raise the pH. When the pH is raised to about 8.5, the current in the switch circuit decreases below 45 mA, the addition of NaOH is then stopped. This smart pH self-adjusting system is set to adjust the pH value of the solution in the range of 0 to 8.5. The practically measured pH range of the solution is in the range of about 0−11 as shown in Figure 5d. The pH value is measured using a pH meter (PHS-3E, Rex) for 2 mL solution taken out from the baker employed using a pipet in a time span of 30 s. It is not needed to stop the system while the measurement is conducted. The excess range of the pH can be attributed to the rapid addition of NaOH and the response time (several seconds) of the PANI dedoping process.[60] Eventually, the smart system shows the promising potential of the layer-structured Ag-NW/PANI composite films as high performance switches in practical pH-responding applications owing to their very high switching ratio and the excellent EC.

CONCLUSION

In summary, the sensitive pH-triggered electrical switch with a much higher switching ratio compared to other switches reported previously has been successfully developed using a layer-structured Ag-NW/PANI composite film prepared *via* an easy vertical spinning method. The layer-structured Ag-NW/PANI nanocomposite film shows a reasonable sensitivity as switch owing to its high switching ratio and the high EC of the Ag-NW layer. Finally, a smart system is demonstrated to achieve a self-adjustment ability of the environmental pH by employing the layer-structured composite film switch. The successful demonstration of the layer-structured nanocomposite film as a pH-responsive switch shows its promising potential application in various pH-relative smart responding systems.

MATERIALS AND METHODS

Materials. All reagents, including aniline, ammonium persulfate (APS), HCl, $NH_3 \cdot H_2O$, $AgNO_3$, $FeCl_3 \cdot 6H_2O$, ethylene glycol and *N*-methyl-2-pyrrolidone (NMP), are in analytical grade and are used as received. All the above raw materials were purchased from Beijing Chemical Works, Beijing, China.

Synthesis of PANI-Emeraldine Base Form (EB) Powders. Emeraldine salt form of PANI was synthesized from a chemical oxidation of aniline with APS oxidant in 1.5 M HCl solution at 0 °C. Emeraldine base form of PANI was obtained by dedoping the emeraldine salt form with 25 wt % ammonia solution for 24 h and was then washed with alcohol for several times and dried in a vacuum for 48 h at 60 °C.

Synthesis of silver nanowires. Silver nanowires were synthesized by a solvothermal method. 1.7 g of $AgNO_3$ was dissolved in 100 mL of ethylene glycol to form solution A. 1.6 g of PVP was dissolved in another 100 mL of ethylene glycol and 2.7 mg of $FeCl_3 \cdot 6H_2O$ was added to form solution B. Then solution B was added to solution A dropwise with vigorous stirring. After that, the mixture was moved to an autoclave and heated to 160 °C for 3 h. Finally, the silver nanowires were obtained by rinsing with a large amount of acetone.

Conflict of Interest: The authors declare no competing financial interest.

Acknowledgment. This work is supported by National Natural Science Foundation of China (No. 11002142, 51373187 and 11372312)

Supporting Information Available: Video of a typical pH self-adjusting process of the smart system, characterization of silver nanowires, and details of evaluation of the contact resistance between Ag-NW layer and PANI layer. This material is available free of charge *via* the Internet at http://pubs.acs.org.

REFERENCES AND NOTES

1. Yoshida, M.; Lahann, J. Smart Nanomaterials. *ACS Nano* **2008**, *2*, 1101–1107.
2. Duan, X.; Xiao, J.; Yin, Q.; Zhang, Z.; Yu, H.; Mao, S.; Li, Y. Smart pH-Sensitive and Temporal-Controlled Polymeric Micelles for Effective Combination Therapy of Doxorubicin and Disulfiram. *ACS Nano* **2013**, *7*, 5858–5869.
3. Walker, D. M.; Tordesillas, A.; Nakamura, T.; Tanizawa, T. Directed Network Topologies of Smart Grain Sensors. *Phys. Rev. E: Stat., Nonlinear, Soft Matter Phys.* **2013**, *87*, 032203.
4. Cherenack, K.; Zysset, C.; Kinkeldei, T.; Munzenrieder, N.; Troster, G. Woven Electronic Fibers with Sensing and Display Functions for Smart Textiles. *Adv. Mater.* **2010**, *22*, 5178–5182.
5. Kelly, F. M.; Meunier, L.; Cochrane, C.; Koncar, V. Polyaniline: Application as Solid State Electrochromic in a Flexible Textile Display. *Displays* **2013**, *34*, 1–7.
6. Hamner, K. L.; Alexander, C. M.; Coopersmith, K.; Reishofer, D.; Provenza, C.; Maye, M. M. Using Temperature-Sensitive Smart Polymers to Regulate DNA-Mediated Nanoassembly and Encoded Nanocarrier Drug Release. *ACS Nano* **2013**, *7*, 7011–7020.
7. Li, Y.; Gao, G. H.; Lee, D. S. pH-Sensitive Polymeric Micelles Based on Amphiphilic Polypeptide as Smart Drug Carriers. *J. Polym. Sci., Polym. Chem.* **2013**, *51*, 4175–4182.
8. Zhang, H. C.; Tian, Y.; Jiang, L. From Symmetric to Asymmetric Design of Bio-Inspired Smart Single Nanochannels. *Chem. Commun.* **2013**, *49*, 10048–10063.
9. Liu, K. S.; Tian, Y.; Jiang, L. Bio-Inspired Superoleophobic and Smart Materials: Design, Fabrication, and Application. *Prog. Mater. Sci.* **2013**, *58*, 503–564.
10. Mao, Y.; Bao, Y.; Yan, L.; Li, G.; Li, F.; Han, D.; Zhang, X.; Niu, L. pH-Switched Luminescence and Sensing Properties of a Carbon Dot-Polyaniline Composite. *RSC Adv.* **2013**, *3*, 5475–5482.
11. Raymond, O.; Font, R.; Suarez-Almodovar, N.; Portelles, J.; Siqueiros, J. M. Frequency-Temperature Response of Ferroelectromagnetic Pb(Fe1/2Nb1/2)O-3 Ceramics Obtained by Different Precursors. Part I. Structural and Thermoelectrical Characterization. *J. Appl. Phys.* **2005**, *97*, 084107.
12. Yun, C.; You, J.; Kim, J.; Huh, J.; Kim, E. Photochromic Fluorescence Switching From Diarylethenes and Its Applications. *J. Photochem. Photobiol., C* **2009**, *10*, 111–129.
13. Ko, J. H.; Yeo, S.; Park, J. H.; Choi, J.; Noh, C.; Son, S. U. Graphene-Based Electrochromic Systems: the Case of Prussian Blue Nanoparticles on Transparent Graphene Film. *Chem. Commun.* **2012**, *48*, 3884–3886.
14. Lampen, P.; Bingham, N. S.; Phan, M. H.; Kim, H.; Osofsky, M.; Pique, A.; Phan, T. L.; Yu, S. C.; Srikanth, H. Impact of Reduced Dimensionality on the Magnetic and Magnetocaloric Response of La0.7Ca0.3MnO3. *Appl. Phys. Lett.* **2013**, *102*, 062414.
15. Kulkarni, M. V.; Kale, B. B. Studies of Conducting Polyaniline (PANI) Wrapped-Multiwalled Carbon Nanotubes (MWCNTs) Nanocomposite and Its Application for Optical pH Sensing. *Sens. Actuators, B* **2013**, *187*, 407–412.
16. Xing, L.; Zheng, H.; Cao, Y.; Che, S. Coordination Polymer Coated Mesoporous Silica Nanoparticles for pH-Responsive Drug Release. *Adv. Mater.* **2012**, *24*, 6433–6437.
17. Lim, E.-K.; Huh, Y.-M.; Yang, J.; Lee, K.; Suh, J.-S.; Haam, S. pH-Triggered Drug-Releasing Magnetic Nanoparticles for Cancer Therapy Guided by Molecular Imaging by MRI. *Adv. Mater.* **2011**, *23*, 2436–2442.
18. Li, S.; Zheng, J.; Chen, D.; Wu, Y.; Zhang, W.; Zheng, F.; Cao, J.; Ma, H.; Liu, Y. Yolk-Shell Hybrid Nanoparticles with Magnetic and pH-Sensitive Properties for Controlled Anticancer Drug Delivery. *Nanoscale* **2013**, *5*, 11718–11724.
19. Bigall, N. C.; Curcio, A.; Leal, M. P.; Falqui, A.; Palumberi, D.; Di Corato, R.; Albanesi, E.; Cingolani, R.; Pellegrino, T. Magnetic Nanocarriers with Tunable pH Dependence for Controlled Loading and Release of Cationic and Anionic Payloads. *Adv. Mater.* **2011**, *23*, 5645–5650.
20. Pu, H.-L.; Chiang, W.-L.; Maiti, B.; Liao, Z.-X.; Ho, Y.-C.; Shim, M. S.; Chuang, E.-Y.; Xia, Y.; Sung, H.-W. Nanoparticles with Dual Responses to Oxidative Stress and Reduced pH for Drug Release and Anti-Inflammatory Applications. *ACS Nano* **2014**, *8*, 1213–1221.
21. Mo, R.; Sun, Q.; Xue, J.; Li, N.; Li, W.; Zhang, C.; Ping, Q. Multistage pH-Responsive Liposomes for Mitochondrial-Targeted Anticancer Drug Delivery. *Adv. Mater.* **2012**, *24*, 3659–3665.
22. Yang, X.; Grailer, J. J.; Rowland, I. J.; Javadi, A.; Hurley, S. A.; Matson, V. Z.; Steeber, D. A.; Gong, S. Multifunctional Stable and pH-Responsive Polymer Vesicles Formed by Heterofunctional Triblock Copolymer for Targeted Anticancer Drug Delivery and Ultrasensitive MR Imaging. *ACS Nano* **2010**, *4*, 6805–6817.
23. Nunes, S. P.; Behzad, A. R.; Hooghan, B.; Sougrat, R.; Karunakaran, M.; Pradeep, N.; Vainio, U.; Peinemann, K.-V. Switchable pH-Responsive Polymeric Membranes Prepared *via* Block Copolymer Micelle Assembly. *ACS Nano* **2011**, *5*, 3516–3522.
24. Isojima, T.; Lattuada, M.; Vander Sande, J. B.; Hatton, T. A. Reversible Clustering of pH- and Temperature-Responsive Janus Magnetic Nanoparticles. *ACS Nano* **2008**, *2*, 1799–1806.
25. Lu, Y.; Sarshar, M. A.; Du, K.; Chou, T.; Choi, C.-H.; Sukhishvili, S. A. Large-Amplitude, Reversible, pH-Triggered Wetting Transitions Enabled by Layer-by-Layer Films. *ACS Appl. Mater. Interface* **2013**, *5*, 12617–12623.
26. Kim, B.; Hong, D.; Chang, W. V. Swelling and Mechanical Properties of pH-Sensitive Hydrogel Filled with Polystyrene Nanoparticles. *J. Appl. Polym. Sci.* **2013**, *130*, 3574–3587.
27. Ham, M. H.; Paulus, G. L. C.; Lee, C. Y.; Song, C.; Kalantar-zadeh, K.; Choi, W.; Han, J. H.; Strano, M. S. Evidence for High-Efficiency Exciton Dissociation at Polymer/Single-Walled Carbon Nanotube Interfaces in Planar Nano-heterojunction Photovoltaics. *ACS Nano* **2010**, *4*, 6251–6259.
28. Tarver, J.; Yoo, J. E.; Loo, Y.-L. Polyaniline Exhibiting Stable and Reversible Switching in the Visible Extending into the Near-IR in Aqueous Media. *Chem. Mater.* **2010**, *22*, 2333–2340.
29. Kaempgen, M.; Roth, S. Transparent and Flexible Carbon Nanotube/Polyaniline pH Sensors. *J. Electroanal. Chem.* **2006**, *586*, 72–76.
30. Bober, P.; Lindfors, T.; Pesonen, M.; Stejskal, J. Enhanced pH Stability of Conducting Polyaniline by Reprotonation with Perfluorooctanesulfonic Acid. *Synth. Met.* **2013**, *178*, 52–55.
31. Yan, L.; Chang, Y.-N.; Yin, W.; Liu, X.; Xiao, D.; Xing, G.; Zhao, L.; Gu, Z.; Zhao, Y. Biocompatible and Flexible Graphene Oxide/Upconversion Nanoparticle Hybrid Film for Optical pH Sensing. *Phys. Chem. Chem. Phys.* **2014**, *16*, 1576–1582.
32. Kong, F.; Liu, C.; Song, H.; Xu, J.; Huang, Y.; Zhu, H.; Wang, J. Effect of Solution pH Value on Thermoelectric Performance of Free-Standing PEDOT:PSS Films. *Synth. Met.* **2013**, *185*, 31–37.
33. Zhao, D.; Guo, X.; Gao, Y.; Gao, F. An Electrochemical Capacitor Electrode Based on Porous Carbon Spheres Hybrided with Polyaniline and Nanoscale Ruthenium Oxide. *ACS Appl. Mater. Interface* **2012**, *4*, 5583–5589.
34. Rana, U.; Malik, S. Graphene Oxide/Polyaniline Nanostructures: Transformation of 2D Sheet to 1D Nanotube and *in situ* Reduction. *Chem. Commun.* **2012**, *48*, 10862–10864.
35. Chang, C.-H.; Huang, T.-C.; Peng, C.-W.; Yeh, T.-C.; Lu, H.-I.; Hung, W.-I.; Weng, C.-J.; Yang, T.-I.; Yeh, J.-M. Novel

Anticorrosion Coatings Prepared from Polyaniline/Graphene Composites. *Carbon* **2012**, *50*, 5044–5051.
36. Ge, D.; Yang, L.; Tong, Z.; Ding, Y.; Xin, W.; Zhao, J.; Li, Y. Ion Diffusion and Optical Switching Performance of 3D Ordered Nanostructured Polyaniline Films for Advanced Electrochemical/Electrochromic Devices. *Electrochim. Acta* **2013**, *104*, 191–197.
37. Xiao, H. M.; Zhang, W. D.; Lv, C.; Fu, S. Y.; Wan, M. X.; Mai, Y. W. Large Enhancement in Conductivity of Polyaniline Films by Cold Stretching. *Macromol. Chem. Phys.* **2010**, *211*, 1109–1116.
38. Seger, B.; McCray, J.; Mukherji, A.; Zong, X.; Xing, Z.; Wang, L. An n-Type to p-Type Switchable Photoelectrode Assembled from Alternating Exfoliated Titania Nanosheets and Polyaniline Layers. *Angew. Chem., Int. Ed.* **2013**, *52*, 6400–6403.
39. Lu, J.; Park, B. J.; Kumar, B.; Castro, M.; Choi, H. J.; Feller, J.-F. Polyaniline Nanoparticle-Carbon Nanotube Hybrid Network Vapour Sensors with Switchable Chemo-Electrical Polarity. *Nanotechnology* **2010**, *21*, 255501.
40. Huang, G.-W.; Xiao, H.-M.; Shi, H.-Q.; Fu, S.-Y. Controllable Synthesis of Novel Sandwiched Polyaniline/ZnO/Polyaniline Free-Standing Nanocomposite Films. *J. Polym. Sci., Polym. Chem.* **2012**, *50*, 2794–2801.
41. Yang, Y.; Ouyang, J.; Ma, L. P.; Tseng, R. J. H.; Chu, C. W. Electrical Switching and Bistability in Organic/Polymeric Thin Films and Memory Devices. *Adv. Funct. Mater.* **2006**, *16*, 1001–1014.
42. Bandaru, P. R.; Daraio, C.; Jin, S.; Rao, A. M. Novel Electrical Switching Behaviour and Logic in Carbon Nanotube Y-Junctions. *Nat. Mater.* **2005**, *4*, 663–666.
43. Szot, K.; Speier, W.; Bihlmayer, G.; Waser, R. Switching the Electrical Resistance of Individual Dislocations in Single-Crystalline $SrTiO_3$. *Nat. Mater.* **2006**, *5*, 312–320.
44. Kim, D. C.; Seo, S.; Ahn, S. E.; Suh, D. S.; Lee, M. J.; Park, B. H.; Yoo, I. K.; Baek, I. G.; Kim, H. J.; Yim, E. K.; *et al.* Electrical Observations of Filamentary Conductions for The Resistive Memory Switching in NiO Films. *Appl. Phys. Lett.* **2006**, *88*, 202102.
45. Zhang, H. M.; Wang, X. H.; Li, J.; Mo, Z. S.; Wang, F. S. Conducting Polyaniline Film from Aqueous Dispersion: Crystallizable Side Chain Forced Lamellar Structure for High Conductivity. *Polymer* **2009**, *50*, 2674–2679.
46. Tang, Q. W.; Wu, J. H.; Sun, X. M.; Li, Q. H.; Lin, J. M. Layer-by-Layer Self-Assembly of Conducting Multilayer Film from Poly(Sodium Styrenesulfonate) and Polyaniline. *J. Colloid Interface Sci.* **2009**, *337*, 155–161.
47. Park, J. K.; Kwon, O. P.; Choi, E. Y.; Jung, C. K.; Lee, S. H. Enhanced Electrical Conductivity of Polyaniline Film by a Low Magnetic Field. *Synth. Met.* **2010**, *160*, 728–731.
48. De, S.; Higgins, T. M.; Lyons, P. E.; Doherty, E. M.; Nirmalraj, P. N.; Blau, W. J.; Boland, J. J.; Coleman, J. N. Silver Nanowire Networks as Flexible, Transparent, Conducting Films: Extremely High DC to Optical Conductivity Ratios. *ACS Nano* **2009**, *3*, 1767–1774.
49. Yang, C.; Gu, H.; Lin, W.; Yuen, M. M.; Wong, C. P.; Xiong, M.; Gao, B. Silver Nanowires: From Scalable Synthesis to Recyclable Foldable Electronics. *Adv. Mater.* **2011**, *23*, 3052–3056.
50. Lee, P.; Lee, J.; Lee, H.; Yeo, J.; Hong, S.; Nam, K. H.; Lee, D.; Lee, S. S.; Ko, S. H. Highly Stretchable and Highly Conductive Metal Electrode by Very Long Metal Nanowire Percolation Network. *Adv. Mater.* **2012**, *24*, 3326–3332.
51. Canobre, S. C.; Almeida, D. A. L.; Polo Fonseca, C.; Neves, S. Synthesis and Characterization of Hybrid Composites Based on Carbon Nanotubes. *Electrochim. Acta* **2009**, *54*, 6383–6388.
52. Zengin, H.; Zhou, W. S.; Jin, J. Y.; Czerw, R.; Smith, D. W.; Echegoyen, L.; Carroll, D. L.; Foulger, S. H.; Ballato, J. Carbon Nanotube Doped Polyaniline. *Adv. Mater.* **2002**, *14*, 1480–1483.
53. Ge, J.; Cheng, G.; Chen, L. Transparent and Flexible Electrodes and Supercapacitors Using Polyaniline/Single-Walled Carbon Nanotube Composite Thin Films. *Nanoscale* **2011**, *3*, 3084–3088.
54. Domingues, S. H.; Salvatierra, R. V.; Oliveirab, M. M.; Zarbin, A. J. G. Transparent and Conductive Thin Films of Graphene/Polyaniline Nanocomposites Prepared Through Interfacial Polymerization. *Chem. Commun.* **2011**, *47*, 2592–2594.
55. Feng, X. M.; Li, R. M.; Ma, Y. W.; Chen, R. F.; Shi, N. E.; Fan, Q. L.; Huang, W. One-Step Electrochemical Synthesis of Graphene/Polyaniline Composite Film and Its Applications. *Adv. Funct. Mater.* **2011**, *21*, 2989–2996.
56. Wu, Q.; Xu, Y.; Yao, Z.; Liu, A.; Shi, G. Supercapacitors Based on Flexible Graphene/Polyaniline Nanofiber Composite Films. *ACS Nano* **2010**, *4*, 1963–1970.
57. Salvatierra, R. V.; Cava, C. E.; Roman, L. S.; Zarbin, A. J. G. ITO-Free and Flexible Organic Photovoltaic Device Based on High Transparent and Conductive Polyaniline/Carbon Nanotube Thin Films. *Adv. Funct. Mater.* **2013**, *23*, 1490–1499.
58. Yu, Z. B.; Zhang, Q. W.; Li, L.; Chen, Q.; Niu, X. F.; Liu, J.; Pei, Q. B. Highly Flexible Silver Nanowire Electrodes for Shape-Memory Polymer Light-Emitting Diodes. *Adv. Mater.* **2011**, *23*, 664–668.
59. Lee, C. H.; Lim, H. S.; Kim, J.; Cho, J. H. Counterion-Induced Reversibly Switchable Transparency in Smart Windows. *ACS Nano* **2011**, *5*, 7397–7403.
60. Yoo, S. J.; Cho, J.; Lim, J. W.; Park, S. H.; Jang, J.; Sung, Y.-E. High Contrast Ratio and Fast Switching Polymeric Electrochromic Films Based on Water-Dispersible Polyaniline-Poly(4-Styrenesulfonate) Nanoparticles. *Electrochem. Commun.* **2010**, *12*, 164–167.
61. Meng, Y. N.; Wang, K.; Zhang, Y. J.; Wei, Z. X. Hierarchical Porous Graphene/Polyaniline Composite Film with Superior Rate Performance for Flexible Supercapacitors. *Adv. Mater.* **2013**, *25*, 6985–6990.
62. Tiwari, A. Synthesis and Characterization of pH Switching Electrical Conducting Biopolymer Hybrids for Sensor Applications. *J. Polym. Res.* **2008**, *15*, 337–342.
63. He, H. X.; Zhu, J. S.; Tao, N. J.; Nagahara, L. A.; Amlani, I.; Tsui, R. A Conducting Polymer Nanojunction Switch. *J. Am. Chem. Soc.* **2001**, *123*, 7730–7731.
64. Das, V. D.; Bhat, K. S. A 2-layer Model to Explain the Thickness Dependence of Conductivity and Thermoelectric-Power of Semiconductor Thin-Films and Application of the Model to Pbte Thin-Films. *J. Appl. Phys.* **1990**, *67*, 3724–3727.
65. Joseph, S.; McClure, J. C.; Chianelli, R.; Pich, P.; Sebastian, P. J. Conducting Polymer-Coated Stainless Steel Bipolar Plates for Proton Exchange Membrane Fuel Cells (PEMFC). *Int. J. Hydrogen Energy* **2005**, *30*, 1339–1344.